**Contemporary Engineering Sciences, Vol. 9, 2016, no. 24, 1183 - 1199**
**HIKARI Ltd, www.m-hikari.com**
**http://dx.doi.org/10.12988/ces.2016.67118**

# Numerical and Mathematical Modeling of Unsteady Heat Transfer within a Spherical Cavity: Applications Laser in Medicine

**Adil Bounouar**

Team of modeling and simulation in mechanics and energetics
Faculty of Sciences, Mohamed V University-Rabat, Morocco

**Kamal Gueraoui**

Team of modeling and simulation in mechanics and energetics
Faculty of Sciences, Mohamed V University-Rabat, Morocco

**Mohammed Taibi**

Laboratory of mechanics and energy, Faculty of Sciences Ain chock
Hassan II University-Casablanca, Morocco

**Amale Lahlou**

Department of Economics, Faculty of Law, Economics and Social Sciences
Mohamed V University-Rabat, Morocco

**Mohamed Driouich**

Team of modeling and simulation in mechanics and energetics
Faculty of Sciences, Mohammed V University-Rabat, Morocco

**Mohammed Sammouda**

Team of modeling and simulation in mechanics and energetics
Faculty of Sciences, Mohamed V University-Rabat, Morocco

**Samir Men-La-Yakhaf**

Team of modeling and simulating in mechanics and energetic
Faculty of Sciences, Mohamed V University-Rabat, Morocco

**Mohammed Belcadi**

Team of modeling and simulating in mechanics and energetics
Faculty of Sciences, Mohamed V University-Rabat, Morocco



## Abstract

The main purpose of this work is to establish a numerical and mathematical modeling of heat transfer phenomenon in spherical cavities in order to model biological tissues. The idea of this study is to address the medical need to know the maximum amount of heat that a human tissue can withstand the outside of a treatment session to minimize side effects that a patient may have after hypothermic treatment such as removal of certain tumor by the lasers.
The phenomenon studied is governed by mathematical equations whose numerical resolution allowed the determination of the temperature profile in different layers of the skin (epidermis, dermis, subcutaneous tissue). We have studied the influence of certain parameters of temperature on laser namely: the power, the spot diameter and irradiation time.

**Keywords:** Heat transfer, spherical cavity, finite volume method, mathematical and numerical modeling, laser, tissue environment

## List of symbols

| | |
|---|---|
| $\nu$ | Frequency of the electromagnetic wave |
| $\omega$ | Pulsation of the electromagnetic wave |
| $\lambda$ | Length of the electromagnetic wave |
| c | Speed of light |
| $f_s$ | Femtosecond |
| $k$ | Thermal conductivity |
| $C_p$ | Specific heat |
| $T$ | Temperature |
| $\rho$ | Density |
| r | Radius of the laser beam |
| $\mu_a$ | Absorption coefficient |
| $\mu_s$ | Diffusion coefficient |
| $\gamma$ | Attenuation coefficient |
| I | Laser beam intensity |
| P | Power density |

## Introduction

Scientific and techniques significantly change during the 20th century. Yet it is probably the progress of medicine, started from the 19$^{th}$ century, which are the most spectacular, especially the human consequences they engender: life expectancy is increasing and the population increases. Today, this area reached a level of maturity thanks to the very modern means used, among other, Laser, which revolutionized several medical disciplines.

It is essential that computer simulations have become essential in order to simulate a real and complex physical phenomenon such as laser radiation. They are based on the implementation of theoretical models. Factors to be considered in a laser heating process with a volume of tissue for a period of time are the optical properties (absorption and scattering coefficient which deflects light out of the path of the laser beam) and the thermal parameters (specific heat, thermal conductivity) of a biological tissue. These parameters depend on the nature of the tissue and the light of wavelength [1-6], [11-13].

During intense illumination of a solid target, in particular by a laser, the electromagnetic energy transmitted to the material is converted into heat, which leads to changes in state and thermodynamic transformations in the irradiated material. Thus, this feature of the laser is very important for our work. The Laser is used in many application areas, industry to medicine.

## 1. Characteristics of the laser radiation

### 1.1. Consistency

Temporal coherence is related to the monochromaticity of a light source. The excited atoms from a source emit electromagnetic vibrations in the train as long or short wave. If we consider a wave train duration $T_c$, the length occupied in space by this wave train is $L_c = c\,T_c$ or $L_c$ and $T_c$ are the length and the coherence time. In the case of the laser, the wave trains are much longer than conventional sources [6].

The spatial coherence is a measure of the degree of phase variation along the wave front at different points of this front at a given time. Only coherent waves can interfere.

### 1.2. Divergence

Conventional light sources emit in all directions. Therefore, their intensity decreases with the square root of distance. In the case of the laser, because of the properties of the resonator, there is emission of light only very near and parallel to the optical axis of the cavity [6].

In the case of perfect spatial coherence, the beam of finite dimension inevitably has a divergence due to diffraction. His value $\theta$ is given by the diffraction laws

$\theta = \frac{\beta\,\lambda}{D_o}$ with, $\beta$ is the proportionality factor dependent on the energy distribution in the beam ($\beta \approx 1$), $\lambda$ the beam of the wavelength, and $D_o$ the diameter of the opening diffracting the beam.

### 1.3. Energy distribution, field mode

The intensity distribution in the section of a laser beam controls its energy distribution. The shape of the energy distribution is determined by the resonator configuration (shape mirrors, diameter of the tube opening, etc.)

### 1.4. Power density (intensity) issued

The intensity of the laser beam can be very large because the power output is focused on a very small surface. The determination of the geometrical characteristics of the beam can be done irrespective of the radial distribution of laser intensity I (Energy flux density expressed in $W/cm^2$). The intensity I(r) follows the fundamental mode of the optical cavity. For a fundamental mode TEM 00 (Gaussian) was:

$$I(r) = I_0\ exp\left[-\left(\frac{2r^2}{R_e^2}\right)\right]$$

with,

$I_0 = \frac{f_m\,P}{\pi R_e^2}$ : Power density at beam center,
P : Laser beam power,
$R_e$ : Illumination ray,
$f_m$ : Efficiency ratio of the optical path,
r : Next radius the axis orthogonal to the intensity.

## 2. Action of the laser radiation on matter

When electromagnetic beam intensity $I_0$ ($I_0 = I_{x=0}$) seeps into a solid medium, liquid or gas, the variation in the transmitted intensity I(x) in function of the distance, x, depends on the absorption coefficient, α, middle. The beam intensity decreases according to the Beer- Lambert law [7]:

$$I(x) = I_0 \exp(-\alpha x)$$

with $\alpha = 2\,\omega\,\frac{k}{c}$. According to α, a material can behave in three different ways against its optical properties, either opaque or transparent without loss or semi-transparent.

### 2.1. Process Heat Transfer

The incident $I_0$ intensity laser radiation absorbed at the surface seeps into the environment, causing the decrease in the intensity of the beam according to the Beer- Lambert law [6].

Absorbed to the surface, penetrates inside the medium, causing the decrease of the beam intensity according to Lambert-Beer law [6]. And since the power density $P$ same is written in the form $P = \frac{\partial I}{\partial x}$ then this power is given [13] by : $P(x,t) = (1-R)\, I(t)\, \alpha\, exp(-\alpha x)$.

### 2.2. Interaction laser radiation / fabrics

#### 2.2.1 General characteristics of biological tissue

A biological tissue is a collection of similar cells and the same origin, grouped in clusters, network or beam. A tissue can form a functional unit, which is to say that its cells contribute to a same function. Biological tissues are regenerated regularly and are assembled together to form [8] bodies.
The variation of the temperature and heat transfer depends essentially on thermal properties of the tissue as follows: Thermal conductivity $k$, specific heat $c$, Density $\rho$, thermal diffusivity $D$, emissivity and latent heat.

#### 2.2.2. Thermal conductivity

Thermal conductivity is a characteristic of each material. It indicates the quantity of heat propagating by thermal conduction in 1 second through $1\ m^2$ a thick material of a 1 m, when the temperature difference between the two faces of 1 °K.

#### 2.2.3. Specific heat

It is determined by the amount of energy to be provided by heat exchange to raise a Kelvin temperature of unit mass of a substance. This is an intensive magnitude equal to the heat capacity relative to the mass of the body being studied.

#### 2.2.4. Thermal diffusivity

It measures the penetration of heat by conduction in the material. It is given by $D = \frac{\lambda}{\rho\, C_p}$

#### 2.2.5. Emissivity

The ability of a material to emit heat radiations way is called emissivity. This coefficient of emissivity $\varepsilon$ for any real material has an emissivity of less than 1 ($\varepsilon < 1$) and varies depending on the wavelength of the transmitted signal.

### 2.3. Optical parameters

The most important optical parameters are:

- The absorption coefficient $\mu_a(cm^{-1})$
- The diffusion coefficient $\mu_s(cm^{-1})$ which takes into account the anisotropy of the medium $g$ factor.
- The attenuation global coefficient $\gamma\ (cm^{-1})$ this is the sum of two coefficients and it is also called extinction coefficient $\gamma = \mu_a + \mu_s\,(1-g)$

### 2.4. Different interaction phenomenon

There are several types of interaction between the laser radiation and the affected tissue. These include: reflection, transmission and scattering [13].

When electromagnetic radiation reaches the tissue, certain wavelengths are absorbed while others are reflected by the object. Part of the radiation may optionally be transmitted through the object if it is more or less transparent, with a change of direction of propagation of the refraction. The fraction of radiation that is absorbed modifies the internal energy of the object and produces heat to be re-emitted as radiation of a greater wavelength.

All objects are thus characterized by an coefficient of absorption $\alpha_\lambda$, a coefficient of reflection $\rho_\lambda$, and a coefficient of transmission $\tau_\lambda$, which express respectively the share of energy absorbed, reflected and transmitted to the wavelength λ. These three factors have values ranging from 0 to 1 and their sum is always equal to 1, according to the principle of conservation of energy [13].

$$\alpha_\lambda + \rho_\lambda + \tau_\lambda = 1$$

Once absorbed, the light energy is converted into thermal or mechanical energy. The absorption of light energy is necessary to achieve a therapeutic result. The study of the effects of interaction with biological tissue laser radiation has established that they depend on the conditions of radiation - tissue interaction , that is to say, the duration of exposure ($T_{expos}$), the power ($P_{laser}$), of the wavelength , the nature of the fabric. These parameters are related by the following mathematical formulas [13]:

- $Irradiance = P_{laser} / Surface\ du\ spot$ (Watts/cm$^2$),
- $Fluence = Irradiance \times T_{expos}$ (Joules/cm$^2$),
- $E_{reçue} = P_{laser} \times T_{expos}$ (Joules),
- $E_{reçue} = Irradiance \times Surface\ du\ spot \times T_{expos}$ (Joules).

## 3. Mathematical formulation of our problem

Thermal transfer is a complex process, in the general case, the result of the superposition of three basic modes of transfer: conduction, convection and radiation. In the case of our study, we consider the case of unsteady transfer by conduction in a spherically symmetric cavity modeling the biological tissue, considered a homogeneous and isotropic material.

### 3.1. Equated the phenomenon

The transfer of energy (heat) in each point of the biological tissue subjected to laser radiation is governed by the following heat equation [6]:

$$K\,\Delta T + \overrightarrow{grad}(K)\ \overrightarrow{grad}(T) + P = \rho\, C_p\, \frac{\delta T}{\delta t} \tag{1}$$

where $\Delta$T is the Laplacian of the temperature, P the source term, ρ density, $C_p$ the heat capacity of the material (fabric), K the thermal conductivity and t the time.

### 3.2. Projection of the heat equation

The projection in spherical coordinates through a spherically symmetric cavity ($T = f(r)$) and in the case of a homogeneous isotropic material (K considered constant), equation (1) becomes:

$$K\left[\frac{1}{r^2}\frac{\partial}{\partial r}\left(r^2\frac{\partial T}{\partial r}\right)\right] + P = \rho\, C_p\, \frac{\partial T}{\partial t} \tag{2}$$

The source term P in continuous mode: $P(r) = (1 - R)\, I_0\, \alpha \exp(-\alpha r)$
with,

r: Penetration distance within the material,

α: Absorption coefficient,

$I_0 = \frac{P}{\pi(d/4)^2}$: Power density at the beam center where $d$ is the diameter of the spot,

P: Laser beam power.

## 4. Discretization of equations and solving process

### 4.1. Discretization

The equation of energy transfer (2) cannot be solved analytically in all cases, so recourse to numerical methods is required. For this, we opted for the use of the finite volume method [9]. It integrates the following central control volume $P$ and volume time domain, then the equation is multiplied by $(dt\, dv)$ where $dv = 4\pi\, r^2 dr$, we obtain :

$$\int_{Vc}\int_{t}^{t+\Delta t} K\left[\frac{1}{r^2}\frac{\partial}{\partial r}\left(r^2\frac{\partial T}{\partial r}\right)\right]\ dv\ dt + \int_{Vc}\int_{t}^{t+\Delta t} P\ \ dv\ dt = \int_{Vc}\int_{t}^{t+\Delta t} \rho\ C_p\ \frac{\partial T}{\partial t}\, dv\ dt$$

$$\int_{o}^{e}\int_{t}^{t+\Delta t} K\left[\frac{\partial}{\partial r}\left(r^2\frac{\partial T}{\partial r}\right)\right]\ dr\ dt + \int_{o}^{e}\int_{t}^{t+\Delta t} P\ r^2\ \ dr\ dt = \int_{o}^{e}\int_{t}^{t+\Delta t} \rho\ C_p\frac{\partial T}{\partial t}r^2\ \ dr\ dt$$

$$\int_{o}^{e}\int_{t}^{t+\Delta t} \rho\ C_p\frac{\partial T}{\partial t}r^2\ \ dr\ dt = \int_{t}^{t+\Delta t}\left[\int_{o}^{e} \rho\ C_p\frac{\partial T}{\partial t}\ r^2\ \ dr\right]dt$$

so: $\int_{o}^{e}\ r^2 dr\ = {r_p}^2\Delta r$

from where,

$$\int_{t}^{t+\Delta t}\left[\int_{o}^{e} \rho\ C_p\frac{\partial T}{\partial t}\ r^2\ dr\right]dt = \rho\ \ C_p r_p^2\ \Delta r\ \left(T_p^{t+\Delta t} - T_p^{t}\right)$$

with $T_p^{t+\Delta t}$ is the temperature at time $t+\Delta t$ and $T_p^{t}$ is the temperature at the preceding moment $t$.

$$\int_{o}^{e}\int_{t}^{t+\Delta t} P\ r^2\ \ dr\ dt = \int_{t}^{t+\Delta t}\left[\int_{o}^{e} P\ r^2\ \ dr\right]\ dt = P\ r_p^2\ \Delta r\ \Delta t$$

$$\int_{o}^{e} K\frac{\partial}{\partial r}\left(r^2\frac{\partial T}{\partial r}\right)\ dr = \left[K\ r^2\frac{\partial T}{\partial r}\right]_{o}^{e} = K\left[{r_e}^2\left(\frac{\partial T}{\partial r}\right)_e - {r_o}^2\left(\frac{\partial T}{\partial r}\right)_o\right]$$

with,

$$\left(\frac{\partial T}{\partial r}\right)_e = \frac{T_E - T_p}{\Delta r} \qquad et \qquad \left(\frac{\partial T}{\partial r}\right)_o = \frac{T_p - T_o}{\Delta r}$$

So:

$$\int_{t}^{t+\Delta t}\int_{o}^{e} K\ \frac{\partial}{\partial r}\left(r^2\frac{\partial T}{\partial r}\right)\ dr\ dt = K\int_{t}^{t+\Delta}\left[r_e^2\ \left(\frac{T_E - T_p}{\Delta r}\right) - r_o^2\ \left(\frac{T_p - T_o}{\Delta r}\right)\right]dt$$

$$= K\ \left[r_e^2\ \left(\frac{T_E - T_p}{\Delta r}\right)\Delta t - r_o^2\left(\frac{T_p - T_o}{\Delta r}\right)\Delta t\right]$$

Simplifying yields:

$$K\ r_e^2\ \left(\frac{T_E - T_p}{\Delta r}\right)\Delta t - K\ r_o^2\ \left(\frac{T_p - T_o}{\Delta r}\right)\Delta t + P\ r_p^2\ \Delta r\ \Delta t = \rho\ \ C_p\ r_p^2\ \Delta r\left(T_p - T_p^0\right)$$

By arranging combinations of terms:

$$T_p^{t+\Delta t}\left(\frac{\Delta t}{\Delta r}\ K\ r_e^2 + \frac{\Delta t}{\Delta r}\ K\ r_o^2 + \rho\ \ C_p\ r_p^2\ \Delta r\right)$$

$$= \frac{\Delta t}{\Delta r}\ K\ r_e^2\ T_E^{t+\Delta t} + \frac{\Delta t}{\Delta r}\ K\ r_o^2\ T_o^{t+\Delta t} + P\ r_p^2\ \Delta r\ \Delta t + \rho\ \ C_p r_p^2\ \ \Delta r\ \ T_p^t$$

This equation can be expressed in the following form:

$$a_p\, T_p^{t+\Delta t} + a_E\, T_E^{t+\Delta t} + a_O\, T_O^{t+\Delta t} = d$$

Or,

$$a_i\, T_i^{k+1} + a_{i+1}\, T_{i+1}^{k+1} + a_{i-1}\, T_{i-1}^{k+1} = d_i^k \tag{3}$$

with,

$$\begin{cases} a_p &= \dfrac{\Delta t}{\Delta r}\, K\, (r_e^2 + r_o^2\,) + \rho\;\; C_p\, r_p^2\, \Delta r \\ a_E &= -\dfrac{\Delta t}{\Delta r}\, K\, r_e^2 \\ a_O &= -\dfrac{\Delta t}{\Delta r}\, K\, r_o^2 \\ d &= P r_p^2\, \Delta r\, \Delta t + \rho\, C_p\, r_p^2\, \Delta r\, T_p^t \\ r_e &= \dfrac{r_E + r_p}{2} \\ r_O &= \dfrac{r_O + r_p}{2} \end{cases}$$

**4.2. Resolution process**

Solving the algebraic equation (3) is made by the double scanning method [14-27]. The equation for the temperature is:

$$A(i)T(i-1) + B(i)\,T(i) + C(i)\,T(i+1) = D(i)$$

Let: $T(i) = \alpha(i)T(i+1) + \beta(i)$ is:

$$T(i-1) = \alpha(i-1)T(i) + \beta(i-1)$$

It comes:

$$A(i)\alpha(i-1)T(i) + B(i)T(i) + C(i)T(i+1) + A(i)\beta(i-1) = D(i)$$

This equation can be put in the form:

$$T(i) = \frac{-C(i)}{B(i) + A(i)\,\alpha(i-1)}T(i+1) + \frac{D(i) - A(i)\,\beta(i-1)}{B(i) + A(i)\,\alpha(i-1)}$$

with,

$$\begin{cases} \alpha(i) &= \dfrac{-C(i)}{B(i) + A(i)\,\alpha(i-1)} \\ \beta(i) &= \dfrac{D(i) - A(i)\,\beta(i-1)}{B(i) + A(i)\,\alpha(i-1)} \end{cases}$$

Recurrences of the above formulas are primed using the data $\alpha(1)$ and $\beta(1)$ from the boundary conditions. The first scan from *i = 2* to $i = i_{max}$, functions is deter-

mined α et β. While during the return scan from $i = i_{max-1}$ to $i = 2$, the temperature $T$ will be determined.

## 5. Boundary conditions and initial profile

### 5.1. Initial profile

The distribution of the temperature within the biological tissue and on the surface is assumed to be known at the instant $= 0 : T(r, t = 0) = T_0$. Generally the initial temperature field is constant, equal to the tissue temperature to the normal state : $T_0 = 37\ °c$.

### 5.2. Boundary conditions

The free surface of the tissue is perfectly insulating, therefore no loss of heat to the surface. This condition resulted in the relationship: $\frac{\partial T(r=0,\ t)}{\partial r} = 0$.

This condition reflects the approximation that there is no heat loss through the free surface of the tissue (adiabatic heating). The interface $(r = R_e)$ is maintained at a uniform temperature equal to $T_0$. We will have at $T_1 = T_2$ : $\alpha(1) = 1$ and $\beta(1) = 0$.

## 6. Results and discussions

The study of thermal heating of biological tissue in order to thermotherapy can predict the evolution of the temperature which is the result of the laser tissue interaction.

To optimize the use of a laser, several parameters must then be controlled such that: the wavelength, the power (continuous wave laser), the diameter of the spot, the beam interaction time and energy of a pulse in the case of a pulsed laser.

We first determine the parameters of pulsed and continuous laser to produce tissue coagulation and then we estimate the spatial and temporal distribution of temperature. To better understand this interaction, we will take the concrete example of treatment of urinary stones by laser, and then we will interpret the results obtained at fair value.

### 6.1. Thermal and optical properties

The human skin consists of three layers: the epidermis, dermis and hypodermis, of respective thicknesses 50, 2400 and 4000 μm.

The thermal and optical properties of each layer are shown in Table 1 [10]. It is noted that for the wavelength of Nd-Yag 1064 nm laser epidermal diffusion coefficient is 2.33 greater than that of the dermis and 3.8 larger than that of the hypodermis. The epidermis absorbs more light than the dermis about 3.3 times the dermis is 20 times more than the hypodermis.

| Properties | | Epidermis | Dermis | hypodermis |
|---|---|---|---|---|
| $k$ | (W $m^{-1}K^{-1}$) | 0.21 | 0.53 | 0.46 |
| $\rho$ | (Kg $m^{-3}$) | 1200 | 1200 | 1200 |
| $c$ | (J $Kg^{-1}$ $K^{-1}$) | 3600 | 3800 | 3800 |
| $\alpha$ | ($m^2$ $s^{-1}$) | 4.86 $10^{-8}$ | 1.16 $10^{-7}$ | 1.10 $10^{-7}$ |
| $\mu a$ | ($cm^{-1}$) | 4 | 1.2 | 0.2 |
| $\mu s$ | ($cm^{-1}$) | 210 | 90 | 55 |
| $g$ | | 0.77 | 0.77 | 0.77 |

**Table 1:** Thermal and optical properties of each layer, Laser Nd-Yag $\lambda = 1064\ nm$ [10]

### 6.2. Variation of the irradiation intensity as a function of the depth of the skin

As mentioned above, the laser beam intensity decreases according to the Beer-Lambert law:

$I(r) = I_0 \exp(-\alpha r)$ with $I_0 = \frac{P}{\pi r_{spot}^2}$. For a laser Nd-Yag wavelength $\lambda = 1064$ nm, the power $P = 2W$ and spot diameter $D = 5$ mm, the above equation becomes rewrites:
$I(r) = 101859.16 \exp(-\alpha r)$. The α values are given in the table above:

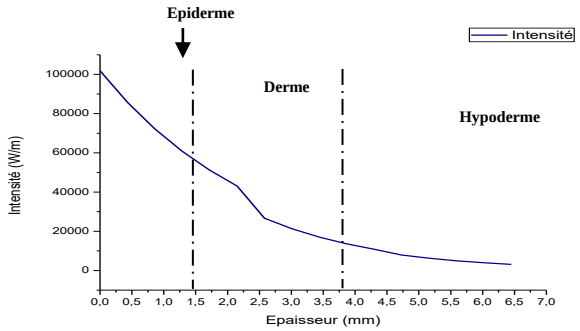


**Figure 1**: Decrease in the intensity of irradiation according to the depth $r$

### 6.3. Profile of temperature in function of medium

Figures 2, 3 and 4 illustrate the temperature profiles as a function of radius for a laser irradiation having the following properties: $P = 2W$, $D = 5mm$ *and* $t = 1s$.

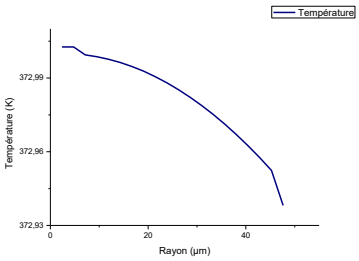


**Figure 2:** The temperature profile epidermal

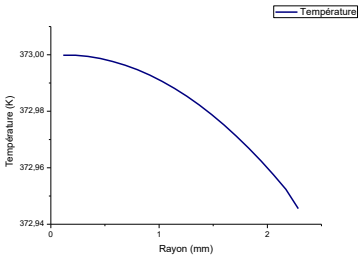


**Figure 3:** The temperature profile dermal

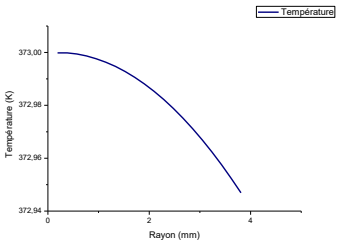


**Figure 4:** The temperature profile hypodermis

### 6.4. The temperature profile function of time

The curves in Figure 5, 6 and 7 show the change in temperature upon exposure to the laser power $P = 2W$ and diameter $5mm$ spot for a duration of one second.

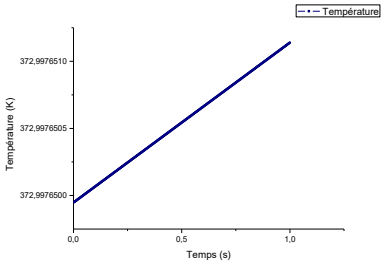


**Figure 5:** The temperature profile epidermal

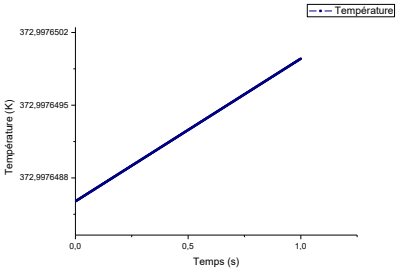


**Figure 6:** The temperature profile Dermal

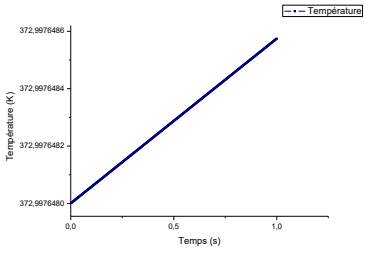


**Figure 7:** The temperature profile hypodermis

It can be seen in Figures 2, 3 and 4 that the end temperature of the laser interaction - skin decreases while penetrating successively in the three layers of the skin. However, the temperature rises linearly with time (Figures 5, 6 and 7).

Temporal changes in temperature are obtained at each point of the area studied. In this sense, the figures (Figure 5, 6 and 7) show a sharp linear increase in temperature versus time for a power of $2W$ , a constant spot diameter equal to $5\ mm$ and equal irradiation time 1s to reach high values favor the coagulation of the tissue. After stopping the laser exposure, the temperature will decrease to its normal temperature of the tissue ($37°c \approx 310\ K$).

### 6.5. Influence of the parameters of the laser beam in case of a Nd-Yag laser continuously

#### 6.5.1. The temperature variation depending on the power

Initially, we will set for a Nd-Yag continuous ($\lambda = 1064$ nm) the spot diameter at $0.5\ cm$, the interaction time is $1.5\ s$ and perform the same operation for $1\ s$ interaction times and $0.5\ s$ .

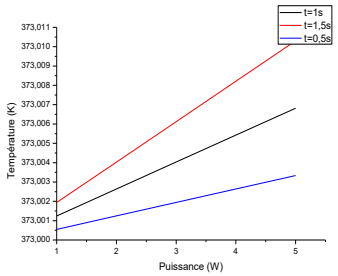


**Figure 8 :** epidermal

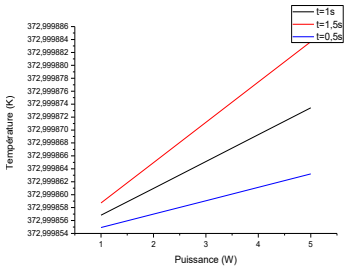


**Figure 9 :** dermal

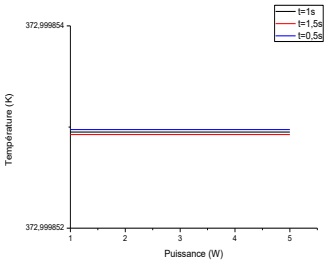


**Figure 10 :** hypodermis

Figures 8 and 9 show the evolution of the linear temperature versus power, the epidermis and dermis. One can notice when the power $P$ increases the fluence increases (particle flow), so the absorption by tissue becomes strong and this pigment shows a very high heat flow. Furthermore, in Figure 10, the temperature of the hypodermis remains almost constant when the power is increased (1 to $5W$) and the processing time by the laser ($0.5s$ to $1.5s$).

### 6.5.2. Variation of the temperature versus spot diameter

In this part, we vary the spot diameter and the length of interaction ($1.5\ s$ , $1\ s$ and $0.5\ s$) for the same laser (Nd-Yag continuous ($\lambda = 1064$ nm)) is setting the power $2W$.

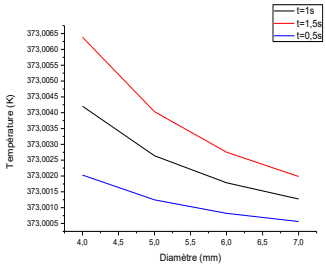


**Figure 11 :** epidermal

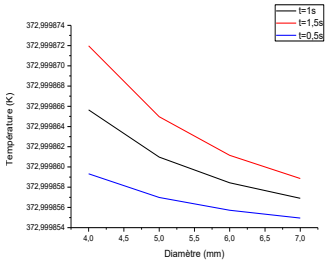


**Figure 12 :** dermal

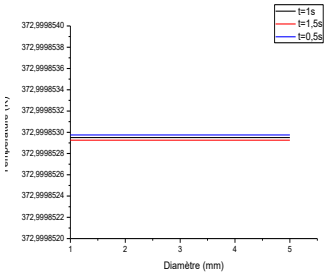


**Figure 13 :** hypodermis

Figures 11 and 12 show the temperature variation depending on the diameter of the fabric for different times of irradiations. It is noted that the temperature varies inversely with respect to the spot diameter this is due to irradiance which is inversely proportional to the square of the spot diameter. However, in Figure 13, the temperature remains almost constant at the hypodermis when the diameter is increased (from 4 to 7 $mm$) and the processing time by the laser ($0.5s$ to $1.5s$).

## Conclusion

The objective of this work is the modeling of thermal diffusion processes in biological tissues. We presented the results of numerical solution of the heat

equation. Since seeks therapeutic solutions via laser, our choice focused on the Nd-Yag laser. We opted for the choice; in the case of treatment of coagulation of a tissue such as hemangiomas; the Nd-Yag laser continuously 1064nm wavelength. This choice was motivated by the fact that such a laser has a good penetration into the tissue. Also, it can be used on black skins by against; it is less absorbed by melanin.

The results obtained in this study are a direct application in the medical field and can be further optimized and expanded; you just have to know the thermal and optical parameters of the tissue environment. In this work, the quantitative and qualitative study of the heat distribution in biological tissue was mandatory for therapeutic hyperthermia, which is expressed mathematically by a numerical simulation of hyperthermia treatments.

## References

[1] M.H. Belghazi, *Modélisation Analytique du Transfert de la Chaleur Dans un Matériau Bicouche en Contact Imparfait et Soumis à une Source de Chaleur en Mouvement*, Université de Limoges, 2008.

[2] L.V. Belle, *Analyse, Modélisation et Simulation de L'apparition de Contraintes en Fusion Laser Métallique*, INSA de Lyon, 2015.

[3] F. Balembois and S. Forget, *Le laser: fondamentaux; lasers et optique non linéaire, Optique pour l'ingénieur*, 2007.

[4] S. Faure, *Etude de L'interaction Rayonnement-matière dans un Milieu Granulaire en vue de L'application au Procédé de Frittage Laser, Matériaux Céramiques et Traitements de Surface,* Ecole Nationale Supérieure de Céramique Industrielle, Thèse 26, 2004.

[5] C.F. Bohren, R. Huffman, *Absorption and Scattering of Light by Small Particles*, éd. Wiley-Interscience, 1983.

[6] M. Belcadi, *Modélisation Théorique et Numérique de l'usinage de l'Alumine par Combinaison du Laser et Micro-ondes*, Thèse de Doctorat, Université Mohamed V, 2015.

[7] A. Nordström, *Determination of the Optical Properties of a Paperboard Packaging Material for Laser Applications*, Tetra Pak Packaging Solutions AB Development and Engineering and Atomic Physics Division Lund Institute of Technology, 2007.

[8] J.M. Brunetaud, *Les mécanismes d'interaction laser - tissus vivants*, 2002.

[9] S. Gabay, G. W. Lucassen, W. Verkruysse, M. J. C. van Gemert, Modeling the Assessment of port wine stain parameters from skin surface temperature following a diagnostic laser pulse, *Lasers in Surgery and Medicine*, **20** (1997), 179-187. http://dx.doi.org/10.1002/(sici)1096-9101(1997)20:2<179::aid-lsm9>3.0.co;2-n

[10] M.V. Allmen, *Laser-Beam Interactions with Materials*, Springer Berlin Heidelberg, 1987. http://dx.doi.org/10.1007/978-3-642-97007-8

[11] W.J. Chang and T.H. Fang, Modelling of solid- liquid interface during laser processing using inverse methodology, *App. Phys. B*, **80** (2005), 373-376. http://dx.doi.org/10.1007/s00340-005-1740-6

[12] M. Kervella, T. Tarvainen, A. Humeau and J. P. L'Huillier, Comparaison de deux modèles hybrides simulant la propagation de la lumière dans les tissus biologiques, *IRBM*, **28** (2007), 80-85. http://dx.doi.org/10.1016/j.rbmret.2007.05.001

[13] M. Benhamouda, *Etude, Conception et Modélisation de la Diffusion de la Chaleur dans les Tissus Biologiques*, Thèse de Doctorat de l'Université du Québec à Trois-Rivières, 2015.

[14] M. Driouich, K. Gueraoui, Y.M. Haddad, M. Sammouda, A. El Hammoumi, M. Kerroum, M. Taibi and O. Fassi Fehri, Numerical and Theoretical Modeling of Unsteady flows for incompressible Fluid in Rigid Conducts. Application to Molten polymers Flow, *International Review on Modeling and Simulations*, **3** (2010), no. 6.

[15] M. Sammouda, K. Gueraoui, M. Driouich, A. El Hammoumi and A. Iben Brahim, The Variable Porosity Effect on the Natural Convection in a Non-Darcy Porous Media, *International Review on Modeling and Simulations*, **4** (2011), no. 5.

[16] M. Driouich, K. Gueraoui, M. Sammouda and Y.M. Haddad, A New Numerical Code to Study the Flow of Molten Polymers In Elastic Pipes, *AES-ATEMA International Conference Series - Advances and Trends in Engineering Materials and their Applications*, (2011).

[17] M. Driouich, K. Gueraoui, M. Sammouda, Y.M. Haddad and I. Aberdane, The Effect of Electric Field on the Flow of a Compressible Ionized Fluid in a Cylindrical Tube, *Adv. Studies Theor. Phys.*, **6** (2012), no. 14, 687-696.

[18] M. Driouich, K. Gueraoui, M. Sammouda and Y.M. Haddad, The Effect of the Rheological Characteristics of the Molten Polymer on its Flow in Rigid Cylindrical Tubes, *Adv. Studies Theor. Phys.*, **6** (2012), no. 12, 569-586.

[19] M. Sammouda, K. Gueraoui, M. Driouich, A. El Hammoumi and A. Iben Brahim, Non-Darcy Natural Convection Heat Transfer Along a Vertical Cylinder Filled by a Porous Media with Variable porosity, *International Review of Mechanical Engineering,* **6** (2012), no. 4, 698-704.

[20] M. Sammouda, K. Gueraoui, M. Driouich, A. Ghouli and A. Dhiri, Double diffusive natural convection in non-darcy porous media with non-uniform porosity, *International Review of Mechanical Engineering,* **7** (2013), no. 6.

[21] R. Chammami, M. Taibi, M. Hami, H. Amar, M. Kerroum, K. Gueraoui and G. Zeggwagh, Influence de la nature de la paroi sur un modèle d'écoulements pulsés de fluides diphasiques. Application à la microcirculation, Influence of the kind of duct on two-fluid pulsatile flows model. Application to the microcirculation, *Houille Blanche,* (2001), no. 3-4, 18-24. http://dx.doi.org/10.1051/lhb/2001030

[22] M. Taibi, R. Chammami, M. Kerroum, K. Gueraoui, A. El Hammoumi and G. Zeggwagh, Modélisations des écoulements pulsés à deux phases, en conduites déformables ou rigides, Pulsating flow of two phases in deformable or rigide tubes, *ITBM-RBM,* **23** (2002), 149-158. http://dx.doi.org/10.1016/s1297-9562(02)80012-2

[23] I. Aberdane, K. Gueraoui, M. Taibi, A. Ghouli, A. El Hammoumi, M. Cherraj, M. Kerroum, M. Walid, O. Fassi Fihri and Y.M. Haddad, Two Dimensional Theoretical and Numerical Approach of pollutant transport in the Lowest Layers of the Atmosphere, *International Review of Mechanical Engineering,* **3** (2009), no. 4.

[24] F. El Khaoudi, K. Gueraoui, M. Driouich and M. Sammouda, Numerical and Theoretical Modeling of natural convection of nanofluids in a vertical rectangular cavity, *International Review on Modeling and Simulations,* **7** (2014), no. 2. http://dx.doi.org/10.15866/iremos.v7i2.585

[25] S. Men-La-Yakhaf, K. Gueraoui and M. Driouich, New numerical and mathematical code reactive mass transfer and heat storage facilities of Argan waste, *Advanced Studies in Theoretical Physics,* **8** (2014), no**.** 10, 485-498. http://dx.doi.org/10.12988/astp.2014.4331

[26] S. Men-la-yakhaf, K. Gueraoui, A. Maaouni and M. Driouich, Numerical and mathematical modeling of reactive mass transfer and heat storage

installations of Argan waste, *International Review on Modeling and Simulations*, **8** (2014), no. 1. http://dx.doi.org/10.15866/ireme.v8i1.1265

[27] K. Gueraoui, A. El Hammoumi and G. Zeggwagh, A numerical solution of pulsatile flow of an inelastic fluid through anisotropic porous viscoelastic pipes, *Houille Blanche*, **7** (1998), 13-20.

**Received: July 14, 2016; Published: September 17, 2016**